THE GROWTH AND THE DEATH OF CARBON FULLERENES AND NANOTUBES

D. TOMÁNEK
Department of Physics and Astronomy
Michigan State University
East Lansing, Michigan 48824-1116

Abstract. Calculations based on an *ab initio* total energy functional are used to study the recently discovered all-carbon fullerene clusters, such as the buckyball, and nanotubes. Molecular dynamics simulations show that fullerenes are very resilient when subject to binary collisions or exposed to heat. The growth of multi-shell structures is shown to be aided by covalent bonds between the edges of neighboring shells. The fragmentation dynamics of fullerenes and nanotubes, which proceeds via transformation into carbon chains, provides new insight into the formation process of these intriguing systems.

1. Introduction

The discovery of the stable C_{60} molecule with a spherical hollow cage structure few years ago [1] came as a major surprise, since until then the only stable bulk forms of elemental carbon were believed to be graphite and diamond. The C_{60} molecule, sometimes called "buckyball", turned out to be only a particular representative of the family of "fullerene" molecules, named so for their close resemblance to the geodesic dome structures created by the architect Buckminster Fuller. Later on, it has been found that C_{60} molecules can aggregate to form a molecular crystal. The interest in C_{60} rose dramatically following the successful development of a mass production technique for this system [2].

The resulting research first concentrated on characterizing this molecule and the corresponding solid. Next, spurred by the discovery of superconductivity in the alkali intercalated C_{60} solid [3, 4], substantial effort has

T. P. Martin (ed.), Large Clusters of Atoms and Molecules, 405–422.

been invested in modifying the C_{60} molecule and solid, and in the synthesis of other fullerenes[5]. Ongoing research focuses both on the structural and electronic properties of C_{60}-inspired carbon fullerenes. At present, most emphasis is placed on derivatizing and functionalizing pure-carbon fullerenes, investigating more complex spherical or tubular multi-walled structures ("bucky onions" and nanotubes) [6, 7, 8], synthesizing endohedral fullerene complexes containing encapsulated atoms [9], and C_{60} intercalation compounds containing intercalant atoms in the interstitial sites.

In the following, after presenting an overview of theoretical techniques, I will address from the point of view of theory the growth and the disintegration of fullerenes and nanotubes. One of my objectives will be to show that presently available *ab initio* techniques can provide quantitative understanding not only of the stability, but also the dynamics of growth and disintegration of these systems. Even more important, I will try to summarize the microscopic insight obtained using these calculations, which will allow to isolate the essential physics and to find good models which generalize the *ab initio* results to other systems.

2. Theoretical methods

2.1. DENSITY FUNCTIONAL FORMALISM

The most powerful *ab initio* technique used to calculate ground state properties of clusters containing tens to hundreds of atoms, such as modified buckyballs and nanotubes, is the Density Functional Theory (DFT) [10]. This formalism is based on the Kohn-Sham theorem stating that in the ground state, the total electronic energy of a given system is a unique functional of the total charge density $\rho(\vec{r})$. The physical charge density can be obtained by minimizing the functional

$$E[\rho] = T_0[\rho] + \int d\vec{r}\, \rho(\vec{r}) V_{ext}(\vec{r}) + E_H[\rho] + E_{xc}[\rho] = min. \qquad (1)$$

Here, T_0 is the kinetic energy functional, $V_{ext}(\vec{r})$ is the potential of the ions, $E_H[\rho]$ is the Hartree and $E_{xc}[\rho]$ is the exchange-correlation functional. The Density Functional technique is free of parameters, and requires only the knowledge of atomic numbers and atomic positions to determine the total energy and the electron density $\rho(\vec{r})$ of a given system. In the Local Density Approximation (LDA), the nonlocal functional $E_{xc}[\rho]$ is replaced by a local function $\tilde{E}_{xc}(\rho)$ which reproduces the exchange-correlation energy in the homogeneous electron gas exactly. Further simplification is achieved by either freezing in the core electrons in their atomic configurations, or by replacing the ionic potentials by first-principles pseudopotentials which combine the nucleus and the core electrons. For clusters, a local Gaussian

orbital or a numerical basis can be used. Yet even with these simplifications, *ab initio* DFT calculations are computationally very intensive. For this reason, many parametrized techniques compete successfully with this formalism.

2.2. LINEAR COMBINATION OF ATOMIC ORBITALS TECHNIQUE

A computationally efficient way to determine the electronic spectrum and the total energy of large systems is a parametrized Linear Combination of Atomic Orbitals (LCAO) formalism. This one-electron technique provides us with a physically sensible way to extrapolate *ab initio* results to systems with low symmetry. The general expression for the total energy of a carbon cluster is [11, 12]

$$E_{tot} = \sum_i E_{coh}(i) \tag{2}$$

$$= \sum_\alpha n_\alpha \epsilon_\alpha + \sum_{i<j} E_r(\{d_{ij}\}) \,. \tag{3}$$

Here, the electronic states of the cluster have been labeled by α and the atomic sites by i, j. The first term in Eq. (3) is the one-electron molecular orbital energy of the cluster, obtained using two-center Slater-Koster [13] matrix elements in the Hamiltonian. The second term describes nuclear and closed-shell repulsion as well as the electronic "overcounting" terms, which are represented by pairwise repulsive energies $E_r(d)$. A recursion technique treatment [12] of the first term in Eq. (3), which describes the nonlocal many-body interactions in the system, leads to linear scaling of computer resources with the number of particles, and parallelizes naturally on massively parallel computer architectures.

The input information consists of the atomic positions and the energy functional parameters for the LCAO Hamiltonian and the repulsive interactions. The information available as output is the total energy of the system E_{tot}, the molecular orbital wave functions, and the energy eigenvalues ϵ_α. The energy functional parameters have been obtained from a fit to LDA results for C_2, carbon chain, graphite and diamond, and are given in Ref. [11]. The computational efficiency of this approach is of particular advantage when computing structural and electronic properties of very large carbon systems, and in molecular dynamics simulations.

2.3. MOLECULAR DYNAMICS FORMALISM

Molecular dynamics (MD) simulations provide the information about the trajectories of individual atoms, and hence about the time evolution of

cluster geometries. More important, they can also be used to determine thermodynamic properties of these systems as a function of time.

The Lagrangian describing a microcanonical ensemble with a constant number of particles and constant energy is given by

$$\mathcal{L} = \sum_{i=1}^{N} \frac{1}{2} m_i s^2 \dot{\vec{\mathbf{q}}}_{\mathbf{i}}^{\,2} - V(\{\vec{q}_i\}) \,, \tag{4}$$

where $\mathbf{q}_i$ and m_i are the coordinates and the masses of the individual particles, and V is the potential energy of the system.

A canonical ensemble, where the temperature rather than the total energy is constrained, can be described by the Nosé-Hoover Lagrangian [14]

$$\mathcal{L} = \sum_{i=1}^{N} \frac{1}{2} m_i s^2 \dot{\vec{\mathbf{q}}}_{\mathbf{i}}^{\,2} - V(\{\vec{q}_i\}) + \frac{1}{2} Q \dot{s}^2 - (N_f + 1) T_{eq} \ln s \,, \tag{5}$$

where N_f is the number of degrees of freedom, Q is a constant, and s is a virtual degree of freedom describing the energy flow between the system and the external heat bath, kept at the temperature T_{eq}.

The trajectories of the individual particles are obtained by integrating the equations of motion [15]

$$\frac{d}{dt}\left(\frac{\partial L}{\partial \dot{q}_{i\alpha}}\right) - \left(\frac{\partial L}{\partial q_{i\alpha}}\right) = 0 \,, \tag{6}$$

$$\frac{d}{dt}\left(\frac{\partial L}{\partial \dot{\underline{h}}_{\alpha\beta}}\right) - \left(\frac{\partial L}{\partial \underline{h}_{\alpha\beta}}\right) = 0 \,, \tag{7}$$

$$\frac{d}{dt}\left(\frac{\partial L}{\partial \dot{s}}\right) - \left(\frac{\partial L}{\partial s}\right) = 0 \,. \tag{8}$$

3. Dynamics of carbon fullerenes

In this Section, I will illustrate the usefulness of the above formalism to study the growth and disintegration of large carbon structures such as the fullerenes and nanotubes [16]. First, I will discuss the *equilibrium geometry* of small carbon clusters as a function of their size, and the extraordinary stability of fullerenes. These results are crucial, among others, for understanding the conditions which optimize the yield of a particular fullerene in the generator. Next, I will address the extraordinary stability of the rigid, yet still elastic, fullerenes in *binary collisions*. Finally, I will show that cluster fragmentation in inelastic collisions is closely related to *thermally-induced disintegration* of individual fullerenes.

3.1. HOW DO FULLERENES GROW?

In the following, I will discuss the energetic arguments explaining the abundance of closed-shell fullerene structures, in particular the C_{60} "buckyball", in carbon vapors. The equilibrium structures of carbon clusters at $T = 0$ can be determined efficiently using the LCAO Hamiltonian and the simulated annealing technique [11]. The equilibrium geometries, which were obtained in this procedure, included chains, rings, and hollow fullerene cages. For the sake of comparison, we also considered fullerene caps (fragments of a C_{60} molecule) and graphite flakes.

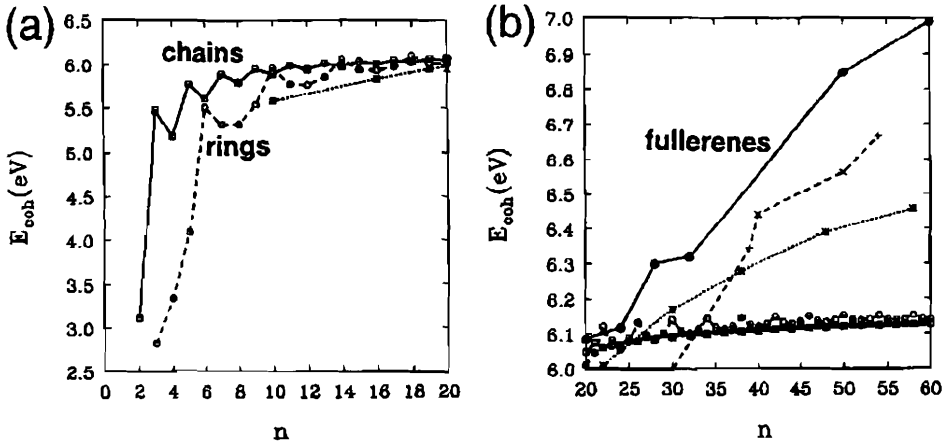

Figure 1. Binding energy per atom E_{coh} in small carbon clusters as a function of cluster size n, (a) for $n \leq 20$ and (b) for $n \geq 20$. Results for chains (□) are connected by a solid line, results for rings (○) are connected by a dashed line, and results for planar graphite flakes (⋆) are connected by a dotted line. Results for buckled fullerene caps with a pentagonal (×) or a hexagonal basis (+) are connected by a dashed line. Results for hollow fullerene cages (•) are connected by a solid line. (From Ref. [11], ©American Physical Society.)

Our results, shown in Figs. 1(a) and (b), indicate an increasing binding energy per atom with increasing cluster size. Based on these total energy results, which are relevant at $T = 0$, the most stable C_n isomers were found to be chains and rings for $n < 20$, in agreement with experimental results [17, 18, 19]. At larger cluster sizes, in particular at $n > 20$, we find rings to be more favorable than chains, since releasing the dangling bond energy of a chain easily offsets the bending energy when forming a ring.

At these larger sizes, however, higher coordinated structures turn out to be energetically much more favorable. For $n > 20$, we find the hollow fullerenes to be the most stable isomers. Also in this size range, the average

binding energy per atom is gradually increasing with increasing fullerene size, approaching the value found in a graphene sheet [20]. At sizes exceeding 700 atoms, finally, multi-walled structures are found to be most stable, due to the significance of the attractive interaction between adjacent walls [20].

A special place among the fullerenes is taken by the C_{60} molecule with its truncated icosahedron structure. It is a hollow cage with a radius of ≈ 3.5 Å, formed by 60 identically equivalent carbon atoms, and hence the most spherical molecule known. The valence charge is delocalized across the surface of the cage, strongly reminiscent of the charge density in a graphite monolayer. This is a consequence of the graphitic sp^2-type bonding in the C_{60} molecule. These strong covalent bonds are responsible for the structural stiffness of this molecule. Nevertheless, the C_{60} does not appear to be exceptionally stable. Since in thermodynamic equilibrium the relative abundance of different clusters should reflect their stability, our results would suggest a continuous size distribution of carbon fullerenes in the mass spectra. This is in clear contrast with the observed abundance of the 60-atom structure. We must conclude that simulations beyond these $T = 0$ stability considerations are necessary to explain the abundance of the "magic" C_{60} cluster in the mass spectra.

3.2. HOW DO FULLERENES DIE IN COLLISIONS?

Next, I will discuss the stability and reactivity of C_n fullerene clusters in binary collisions. Of particular interest in this study was the question of a potential synthesis of more complex structures, such as multi-walled fullerenes (or "bucky onions") [6], by impact-induced encapsulation of the smaller C_{60} buckyball inside the larger C_{240} fullerene. In order to better understand the reaction dynamics, the motion of the individual atoms during the collision process was visualized in a video movie.

Microcanonical molecular dynamics simulations of the collision process were performed at different initial center-of-mass kinetic energies. The C_{60} and the C_{240} clusters were prepared in their equilibrium structures. In the first set of simulations investigating central collisions, the clusters were given an initial linear momentum, zero angular momentum, and the impact parameter was set to zero.

At a low 10 eV center-of-mass kinetic energy, the collision between the C_{240} and the C_{60} clusters could be best characterized as an elastic recoil.

At a ten times higher center-of-mass energy of 100 eV, the C_{240}-C_{60} collision is best described as quasielastic scattering. At the point of impact of C_{60} onto the C_{240} cluster, one can observe a heat- and shock-wave propagating fast within the structure, starting at the point of contact. The C_{240}-C_{60}

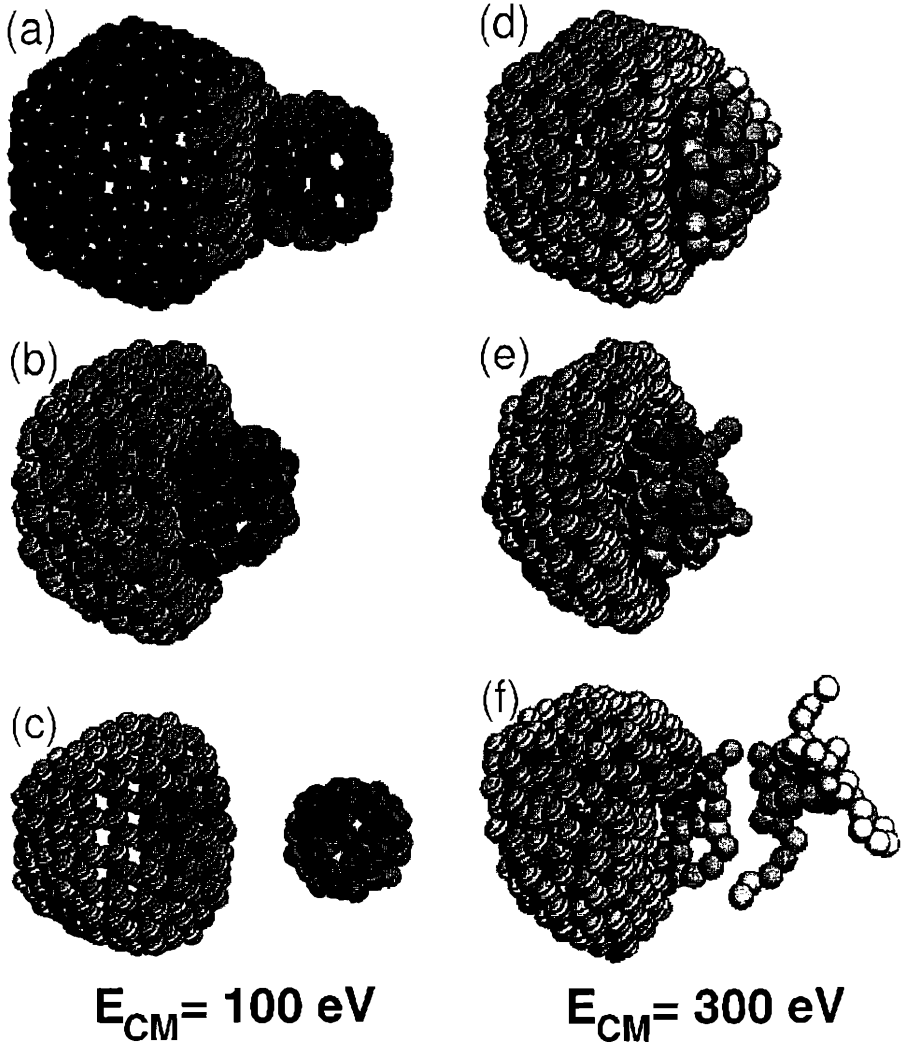

Figure 2. "Snap shots" illustrating the geometry of a C_{60} cluster colliding with a C_{240} cluster at the initial center-of-mass kinetic energy of 100 eV and 300 eV. (From Ref. [21].)

agglomerate is capable of storing the large surplus energy in a substantial structural deformation and the many vibrational degrees of freedom of the system. In spite of the extreme deformations which even result in a negative

Gaussian curvature of the C_{240} cluster, both clusters depart intact, without exchanging any atoms.

Finally, at only three times higher center-of-mass energy of 300 eV, the C_{240}-C_{60} collision leads to an impact-induced fragmentation. The intuitive expectation, that the more rigid C_{60} structure might penetrate the "floppy" wall of the larger C_{240} fullerene, proves to be incorrect. The opposite process occurs — it is the smaller C_{60} cluster which fragments first, leaving the larger C_{240} structure vibrationally highly excited, yet intact. C_{60} is observed to fragment into a structure consisting of linked chains and rings, as well as fragments. A very similar fragmentation dynamics is also observed in simulations assuming a nonzero impact parameter and nonzero initial angular momentum of the fullerenes prior to collision.

The physics underlying this particular fragmentation process is relatively simple. Upon impact, the excessive center-of-mass kinetic energy is distributed into the internal degrees of freedom of both clusters; this vibrational energy appears as heat. The fewer degrees of freedom of the smaller C_{60} cluster experience a higher excitation which results in a higher temperature. Due to the limited amount of vibrational energy which can be stored in the anharmonic potentials, the energy surplus is consumed in the heat of "melting" and partly the heat of "evaporation". The structural transformation of the fragmented C_{60} cluster at high temperatures is driven by the vibrational and structural entropy which is obviously much higher for the floppy one-dimensional chain and ring substructures than the more rigid fullerene structure.

If this explanation is correct, the same structure consisting of linked rings and chains should also occur in *isolated* fullerenes which have been exposed to temperatures beyond those causing melting. As will be shown in the following Subsection, this is indeed the case. More important, this establishes an intriguing link between the impact- and thermally-induced fragmentation of clusters.

3.3. HOW DO FULLERENES DIE IN HEAT?

The present study, originally inspired by the surprising results of the above described inelastic collisions, is intended to answer some fundamental questions related to the nature of thermally induced structural transformations in fullerenes and finite clusters in general. The first important question is, whether atomic clusters – such as fullerenes – undergo *"phase transitions"* such as melting, and what the *"phase diagram"* would look like. Next, one would like to know how to best *characterize* these "phases". Finally, one would like to understand the *driving force* for such "phase transitions".

These and some other related questions have been addressed in a Nosé-

Hoover molecular dynamics simulation of the melting and evaporation process of three prototype fullerenes, namely C_{20}, C_{60}, and C_{240}. The details of the simulation are discussed in Ref. [22]. The results presented below complement nicely those of recent microcanonical ensemble simulations on C_{60} and C_{70} [23].

The key result of the simulation is the total energy of an isolated fullerene as a function of heat bath temperature. In the temperature range of interest, namely between 1,000 K and 10,000 K, the energy E shows a generally linear increase with temperature. The specific heat $c_V = dE/dT$ is generally close to the classical value $c_V = 3k_B$/particle. Strong peaks in the specific heat occur close to 3,000 K and 4,000 K. The peaks get more pronounced with increasing size of the system and, since they are reproducible, can be viewed as a signature of a phase transition which, rigorously speaking, should only occur in an infinite system. Even though the "phase transitions" are gradual in finite systems, the concept of "phases", separated by reproducible features in the specific heat, appears to be useful.

Perhaps the most straight-forward characterization of these "phases" can be achieved by capturing the atomic motion on a video movie, or at least by visualizing "snap shots" of the MD simulation, as shown in Fig. 3. Fig. 3(a) shows that the C_{60} molecule keeps its structure at least up to $T = 1,000$ K. After the first "phase transition" just below $T = 3,000$ K, the systems gets "floppy", as shown in Fig. 3(b). At times, C-C bonds break open in this "phase", and rings of carbon atoms open like a valve. Such processes are always reversible; all atoms "know" their equilibrium positions. Beyond the "melting temperature" of $T_M \approx 4,000$ K, the system transforms to a "pretzel" consisting of linked rings, as shown in Fig. 3(c). Experimental evidence for such a transition has recently been obtained from diffusion experiments [18, 19]. At a temperature exceeding 5,000 K, the rings break open, yielding a structure composed of linked chains, shown in Fig. 3(d). As shown in Figs. 3(e) and (f), the continuous structure of this aggregate eventually breaks into smaller fragments. From this point on, the simulations describe a system of chain and ring fragments rather than the thermodynamics of C_{60}.

More meaningful for the characterization of the different "phases" than mere visualization of "snap shots" is the (time-averaged) binding energy distribution in the system, based on the energy decomposition of Eq. (2). This appears to be more meaningful than a discussion of changing coordination numbers which are ill-defined in amorphous systems.

Below the "melting temperature" $T_M \approx 4,000$ K, all atoms are essentially equivalent and their binding energy is characterized by a single peak in the distribution near 7 eV. This peak broadens and shifts to lower values with increasing temperature. In the "pretzel phase", the binding energy

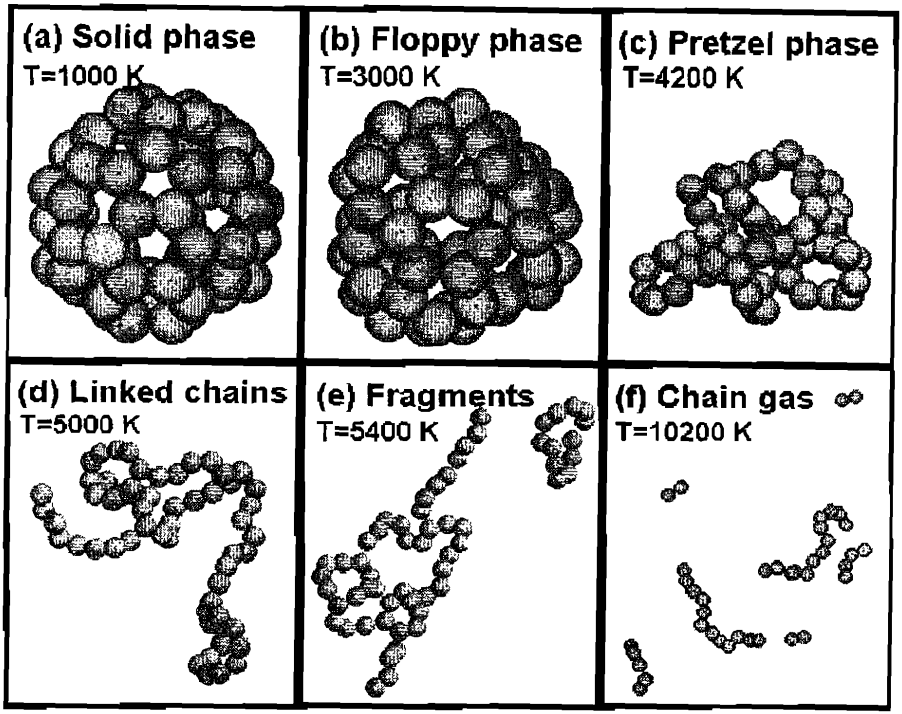

Figure 3. "Snap shots" illustrating the geometry of a C_{60} cluster at temperatures corresponding to the different "phases" discussed in the text. (From Ref. [22], ©American Physical Society.)

distribution changes drastically to a bi-modal distribution which describes the occurrence of two inequivalent types of sites: the twofold coordinated atoms in the strained rings and the more stable multiply-coordinated atoms at the links of these rings. The onset of the "linked chains phase" is marked by a third peak near a binding energy of $\approx$5 eV associated with chain ends. At even higher temperatures, the spectrum broadens and the average stability of the structure decreases.

A simple estimate of the "melting transition" from fullerenes to pretzels can be obtained by comparing the free energies of the two structures which must be equal at the melting point. At this temperature, the larger entropy must outweigh the lower stability of the pretzel structure. The Nosé-Hoover simulations contain the information about the heat uptake, and hence the entropy associated with the atomic degrees of freedom (struc-

tural, vibrational and rotational entropy). A comparison between the entropy of a fullerene and a linear chain (with equal numbers of atoms) indicates a nearly constant entropy difference $\Delta S \approx 2k_B$ (per atom) between these structures [24]. The binding energy difference (per atom) between a fullerene and a chain of ≈ 1 eV leads, together with the above value for the entropy difference, to an estimated "melting temperature" of fullerenes near 5,800 K. This value is of the same order of magnitude as the value obtained in the MD simulation, and also close to the melting point of graphite, $T_M(\text{graphite}) = 3,823$ K [25]. These results confirm that the "melting transition" in fullerenes at $T_M \approx 4,000$ K is driven mainly by the vibrational and structural entropy.

4. Dynamics of carbon nanotubes

Carbon nanotubes were first discovered in a deposit that was forming on the cathode of the carbon arc apparatus used to produce fullerenes [8]. This by-product of the fullerene production soon became the focus of fullerene research [26, 7]. Single-walled carbon nanotubes consist of a single graphene sheet rolled onto itself. By displacing the edges of the graphene sheet along the tube axis before joining them, either achiral or chiral tubes can be formed. Observed multi-walled nanotubes contain several nanotubes nested inside each other, at an average inter-wall separation of 3.4 Å.

The observed multi-walled tubes are believed to grow layer-by-layer in the electric field of the arc. The growth of single-walled tubes, on the other hand, is believed to proceed at the root, near a metal catalyst particle [8, 27, 28]. In the following, I will discuss non-catalytic growth and destruction of carbon nanotubes in the carbon arc.

4.1. HOW DO NANOTUBES GROW?

The recently observed [30] aggregation of carbon atoms into single- and multi-walled nanocapsules (nanotubes terminated by caps from both sides) under homogeneous conditions [31] gave rise to several questions. Why do oblong objects grow, even though spherical objects are more stable [20]? Why do carbon nanotubes grow so long and so perfect? Why are nanotubes so inert? Why do observed nanotubes have predominantly an even number of walls?

The key to answer these questions lies in determining the preferential adsorption site of atoms at the end of a growing nanotube. In the following, I will follow the reasoning of Ref. [30] and discuss two competing growth scenarios for the simplest case, a double-walled achiral nanotube. These scenarios are summarized in Fig. 4. The most reactive sites of a nanotube are at the exposed edges, in particular on the more strained inner tube;

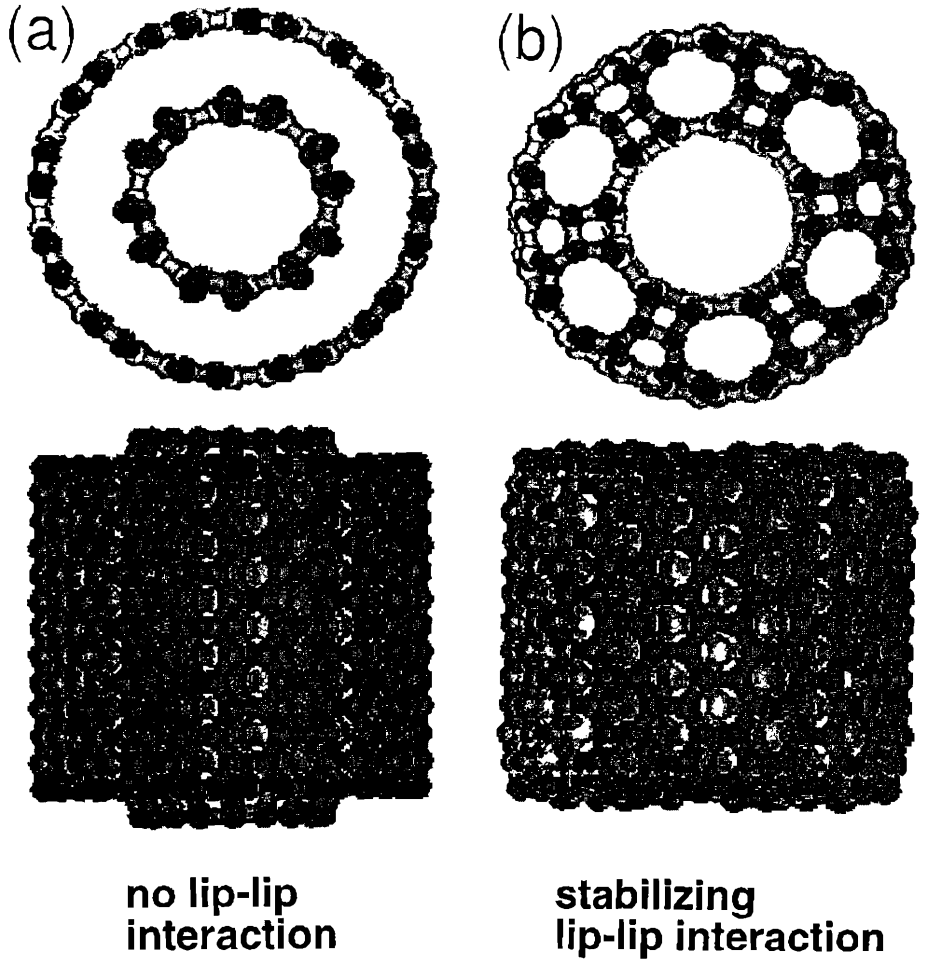

Figure 4. Two possible scenarios for the growth of a double-walled carbon nanotube, shown in top view (top) and side view (bottom). (a) Carbon atoms aggregate on the edge of the inner tube only, saturating the most exposed dangling bonds. (b) Carbon atoms bridge the gap between adjacent carbon nanotubes, saturating the dangling bonds at both tube edges (From Ref. [29].)

they may become the preferential adsorption sites. On the other hand, if aggregating atoms could bridge the gap between adjacent tube edges, they might stabilize the tube end by saturating the dangling bonds at both edges and connect these edges as "spot welds", at the cost of extra strain at the

adjacent tube edges.

To obtain an unbiased answer regarding the preferential growth mechanism, structure optimization and total energy calculations have been performed for an achiral double-walled tube shown in Fig. 4, using the parametrized LCAO formalism [29].

Our results indicate that structures containing "spot welds" between the exposed edges of adjacent tubes [Fig. 4(b)] are energetically favored by $\approx 1.5 - 2.0$ eV per adsorbed carbon atom over structures with these extra atoms on the inner edge only and no such bonds [Fig. 4(a)]. The stabilizing "lip-lip" interaction via covalent "spot welds" has several important consequences which also answer most of the puzzles mentioned above.

The necessary prerequisite for the growth of a long tube rather than a spherical fullerene is a mechanism which would inhibit early dome closure of the tube at the growing end. For a double-walled tube, dome closure due to the insertion of a pentagon defect at the inner wall would occur only at the cost of breaking the covalent "spot welds" connecting the tubes. Hence it is the energy optimization at the growing end rather than global energy considerations which favor growth of long tubes by inhibiting dome closure at only one of the neighboring tube walls. With nonzero probability, two pentagon defects will eventually occur simultaneously at the growing edge of adjacent walls, initiating a double-dome closure. As this probability is rather low, carbon nanotubes tend to grow long.

As saturation of dangling bonds at the growing edge of the nanotubes slows down their growth, defects have time to heal out. This may be an important reason why nanotubes are apparently free of imperfections. The absence of dangling bonds at the growing edge of a double-walled nanotube by carbon "spot-welds" seems to reduce drastically the reactivity of the nanotube with respect to oxygen. Single-walled tubes with unsaturated carbon dangling bonds at the growing edge are known to be etched away rapidly by oxygen.

Once a double-walled nanotube has formed, it can serve as a template for further fattening by growing graphitic overlayers, preferentially arranged as concentric cylinders. Due to the presence of dangling bonds at the growing edge, a single-walled growing outer shell is unlikely to survive in the etching atmosphere of oxygen. A double-walled outer shell, with dangling bonds saturated at the edge, has a much better chance of survival. This may be the reason for a relative abundance of even-numbered walls in multi-shell nanotubes, observed in Transmission Electron Microscopy images [8].

4.2. HOW DO NANOTUBES DIE IN HIGH FIELDS?

The following is a brief review of experimental and theoretical results of Ref. [32] on the disintegration of carbon nanotubes in high electric fields.

Several puzzling phenomena occurred when an isolated carbon nanotube, attached to a commercial graphite fiber, was exposed to an external electric field. *(i)* The emission current was observed to fluctuate in discrete steps. *(ii)* The emission current at high fields was observed to be quenched by laser heating the tip, or by exposing the nanotube to residual gas. *(iii)* A constant dim glow at the tip of the tube was observed, with occasional flare-ups in a much larger region of the whole tube, followed by the same dim glow at the tip.

The key to answer these questions is clearly the microscopic atomic structure at the tip of the nanotube. While a closed dome is energetically preferable at $T = 0$, heating might produce a smooth amorphous structure at the tip, and exposure to large electric fields might even favor formation of sharp structural features ("hair") at the tip. As no direct experimental information is available about the microscopic structure of the nanotube tip under such extreme conditions, we sought for a plausible model which would not only explain all the above phenomena [32], but also be consistent with our theoretical understanding of nanotubes and our molecular dynamics results [29]. The calculations were performed on the simplest system which we expect to exhibit these phenomena, namely a chiral tube with its axis parallel to the applied electric field.

In the infinite field limit, the equilibrium structure of any carbon system, such as a nanotube, is a monatomic carbon "wire", aligned with the field. The energy cost associated with the transformation from a stable structure to a carbon chain is more than compensated by the gain in polarization energy at sufficiently high fields. The energetically least costly mechanism to convert a chiral nanotube into a chain is to unravel it from the end, like a sleeve of a pullover.

The basic assumption in the originally proposed model of a field emitting nanotube [32] is that the tip structure associated with high emission currents contains at least one such monatomic carbon "wire", produced by unraveling the open end of a chiral nanotube. Preliminary results of our molecular dynamics simulations, shown in Fig. 5, indicate that such a monatomic chain is stable at does not reattach to the nanotube at a temperature $T = 2000$ K even in zero applied field. At nonzero fields, this "wire" will be polarized and pulled in the direction of the electric field. At high temperatures, extra stabilization of this "wire" (or any one-dimensional segments in an "imperfect" tip) would come also from the higher entropy associated with the floppier one-dimensional structures. The field emis-

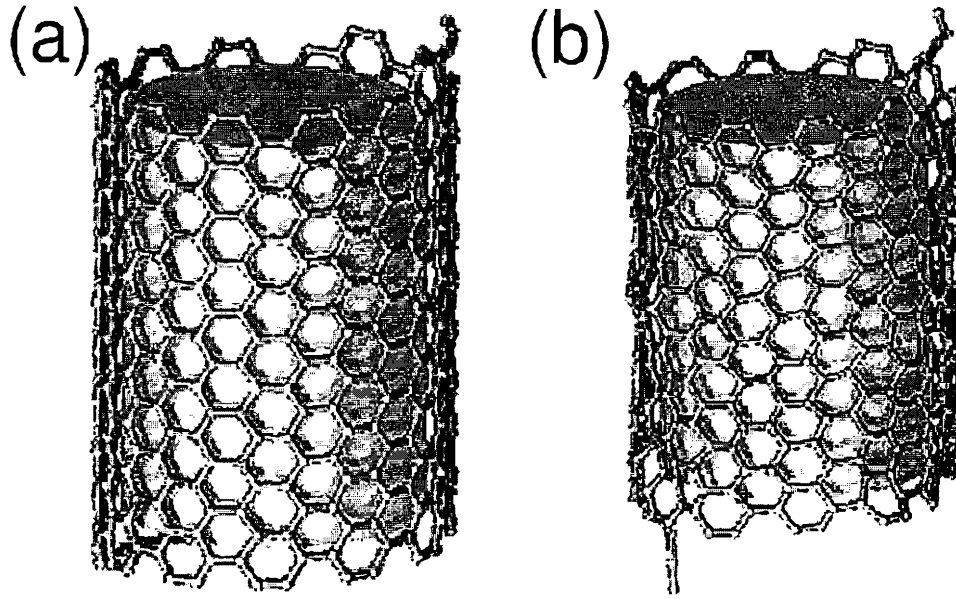

Figure 5. Unraveling of a chiral single-walled nanotube. (a) Optimized $T = 0$ structure with a dangling carbon "wire". (b) At $T = 2000$ K and zero applied field, the dangling carbon "wire" is stabilized by its large vibrational and configurational entropy (From Ref. [29].)

sion currents, observed from a single nanotube, lead us to conclude that monatomic carbon "wires" should be able to sustain currents as high as $i \leq 1$ μA. This value, which appears to be enormous, corresponds roughly to one electron crossing a carbon bond each vibration period of the "wire".

Density functional calculations, performed on a 10-atom carbon chain, indicate an extraordinary stability of this structure in applied fields $E \leq 3$ V/Å. The structure of this monatomic "carbon wire" is closer to that of a cumulenic chain (with all carbon atoms connected by equivalent double-bonds) than to a polyyne (with alternating double/triple bonds, resulting from a Peierls distortion which opens a small gap at the Fermi level).

The postulated monatomic "carbon wire", created by unraveling the open edge of the nanotube, may be the ultimate field emitter [33, 34]. A useful role of the "spot welds" between adjacent walls, discussed in the previous Section, is to terminate the unraveling process once it begins (just like stronger threads in a rip-stop fabric), thus preventing the complete destruction of the nanotube.

The "unraveling model" immediately explains several observed phenomena mentioned above. *(i)* Fluctuation of the emission current in discrete

steps is explained by steady formation and detachment of carbon "wires" from the tip of a multi-walled carbon nanotube. *(ii)* Quenching of the emission current at high fields by exposing the tip to laser heating or residual gas results from detaching or etching away the monatomic "wires" that are responsible for the large current. *(iii)* The observed constant dim glow at the tip results from Ohmic heating and establishes probably the world's smallest Edison light bulb. Occasional flare-ups in a large region of the tube could be caused by a failure of the "spot welds" to terminate the unraveling process, which would results in a catastrophic burn-back of the outermost shell to its base in the nanotube "stalk". If this was not the last shell of a multi-walled tube, the nanotube will continue to glow at the tip as described above.

5. Summary and Conclusions

In this contribution, I presented recent calculations of the equilibrium structure and the dynamics of formation and fragmentation of carbon fullerenes and nanotubes. Theoretical results for *free clusters*, based on *ab initio* and parametrized total energy and molecular dynamics calculations, indicate that

- The *equilibrium structures* of clusters with $N < 20$ carbon atoms are chains and rings, those for $N > 20$ atoms are fullerenes.
- At $T = 0$, the *equilibrium shapes* of free C_n clusters are chains and rings for $n < 20$, spherical fullerene cages for $n > 20$, and multi-walled onions for $n > 700$ atoms. Entropy is expected to play a significant role at $T > 0$.
- The threshold for *inelastic collisions between the C_{240} and the C_{60} fullerenes* is at $E_{CM} \approx 200$ eV. The smaller cluster "melts" upon impact.
- Upon heating, free fullerenes show a *structural transformation* to "pretzels" at $T \approx 4,000$ K, which is driven by vibrational and structural entropy.

In *carbon nanotubes*,

- *The self-assembly of multi-walled tubes* is favored by a stabilizing "lip-lip" interaction between the open ends of adjacent walls. Bridging carbon atoms act as passivating "spot welds".
- In high applied electric fields, chiral nanotubes *disintegrate by unraveling an atomic wire of carbon* from the edge. The driving force is mainly the gain in polarization energy.
- The monatomic carbon "wire" at the tube end is the *"ultimate field emitter"* generating currents up to $i \approx 1$ μA.

Acknowledgement

This work has been performed in collaboration with (alphabetically) Richard Enbody, Philippe Jund, Seong Gon Kim, Michael Schlüter, Richard E. Smalley, and Weiqing Zhong, whose contributions are gratefully acknowledged. Financial support has been provided by the National Science Foundation under Grant No. PHY-8920927, the Air Force Office of Scientific Research under Grant No. F49620-92-J-0523DEF, the Office of Naval Research under Grant Number N00014-90-J-1396, and the organizers of the 1995 NATO Advanced Study Institute on "Large Clusters of Atoms and Molecules" in Erice, Italy.

References

1. H.W. Kroto, J.R. Heath, S.C. O'Brien, R.F. Curl, and R.E. Smalley, Nature **318**, 162 (1985).
2. W. Krätschmer, L.D. Lamb, K. Fostiropoulos, and D.R. Huffman, Nature **347**, 354 (1990).
3. A.F. Hebard, M.J. Rosseinsky, R.C. Haddon, D.W. Murphy, S.H. Glarum, T.T.M. Palstra, A.P. Ramirez, and A.R. Kortan, Nature **350**, 600 (1991).
4. M.J. Rosseinsky, A.P. Glarum, D.W. Murphy, R.C. Haddon, A.F. Hebard, T.T.M. Palstra, A.R. Kortan, S.M. Zahurak, and A.V. Makhija, Phys. Rev. Lett. **66**, 2830 (1991).
5. A. Hirsch, *The Chemistry of the Fullerenes*, (Georg Thieme Publishers, Stuttgart, 1994).
6. Daniel Ugarte, Nature **359**, 707 (1992).
7. T.W. Ebbesen, Ann. Rev. Mater. Sci. **24**, 235 (1994).
8. Sumio Iijima, Nature **354**, 56 (1991); Sumio Iijima, Toshinari Ichihashi, and Yoshinori Ando, Nature **356**, 776 (1992); Sumio Iijima and Toshinari Ichihashi, Nature **363**, 603 (1993).
9. J.R. Heath, S.C. O'Brien, Q. Zhang, Y. Liu, R.F. Curl, H.W. Kroto, and R.E. Smalley, Journal of The American Chemical Society **107**, 7779 (1985).
10. P. Hohenberg and W. Kohn, Phys. Rev. **136**, B864 (1964); W. Kohn and L.J. Sham, Phys. Rev. **140**, (1965).
11. D. Tománek and Michael A. Schluter, Phys. Rev. Lett. **67**, 2331 (1991).
12. W. Zhong, D. Tománek and George F. Bertsch, Solid State Commun. **86**, 607 (1993).
13. J.C. Slater and G.F. Koster, Phys. Rev. **94**, 1498 (1954).
14. W.G. Hoover, Phys. Rev. A **31**, 1695 (1985); S. Nosé, Mol. Phys. **52**, 255 (1984).
15. M.P. Allen and D.J. Tildesley, *Computer Simulation of Liquids* (Oxford, New York, 1990).
16. Synthesis and topology of large fullerenes has been reviewed by Robert F. Curl and Richard E. Smalley in Scientific American, October 1991, p. 54.
17. K.S. Pitzer and E. Clementi, J. Am. Chem. Soc. **81**, 4477 (1961)
18. G. von Helden, N. Gotts, and M.T. Bowers, Nature **363**, 60 (1993).
19. J.M. Hunter, J.L. Fye, E.J. Roskamp, M.F. Jarrold, J. Phys. Chem. **98**, 1810 (1994).
20. D. Tománek, W. Zhong, and E. Krastev, Phys. Rev. B **48**, 15461 (1993).
21. Seong Gon Kim, Weiqing Zhong, and David Tománek, (unpublished).
22. Seong Gon Kim and David Tománek, Phys. Rev. Lett. **72**, 2418 (1994).
23. Eunja Kim, Young Hee Lee and Jae Young Lee, Phys. Rev. B **48**, 18230 (1993).
24. This is true below the "melting point"; both structures are very similar and hence have the same entropy above the "melting point".

25. "CRC Handbook of Chemistry and Physics", 62th edition, CRC Press, Boca Raton, Florida, 1990, p. B-10.
26. R.E. Smalley, Mat. Sci. Eng. **B19**, 1 (1993).
27. D.S. Bethune, C.H. Klang, M.S. De Vries, G. Gorman, R. Savoy, J. Vazquez, and R. Beyers, Nature **363**, 605 (1993).
28. T. Guo, P. Nikolaev, A. Thess, D.T. Colbert, and R.E. Smalley, submitted to Chem. Phys. Lett.
29. David Tománek, Seong Gon Kim, Philippe Jund, Liang Lou, Peter Nordlander, and Richard E. Smalley, (unpublished).
30. Ting Guo, Pavel Nikolaev, Andrew G. Rinzler, David Tománek, Daniel T. Colbert, and Richard E. Smalley, J. Phys. Chem. (1995).
31. In absence of an external electric field, catalytic particles, or a substrate, which were previously believed to be necessary for the generation of nanotubes.
32. A.G. Rinzler, J.H. Hafner, P. Nikolaev, L. Lou, S.G. Kim, D. Tománek, P. Nordlander, D.T. Colbert, and R.E. Smalley, Science (1995).
33. Vu Tien Binh, S.T. Purcell, N. Garcia, J. Doglioni, Phys. Rev. Lett. **69**, 2527 (1992).
34. S. Horch and R. Morin, J. Appl. Phys. **74**, 3652 (1993).